Analysis of Artificial Dielectric Layers with Finite Conductivity

Daniele Cavallo
Microelectronics dept.
Delft University of Technology
Deft, The Netherlands
d.cavallo@tudelft.nl

***Abstract*—Closed-form expressions to describe artificial dielectric layers (ADLs) with finite conductivity are presented. The propagation of a generic plane wave within the artificial material is described by means of transmission line models, where each layer is represented as an equivalent shunt impedance. Since the expressions are derived assuming finite conductivity of the metal, an accurate estimation of the losses within the artificial dielectric is obtained from the equivalent circuit.**

I. Introduction

Modern radar and wireless communication applications are increasing their frequency of operation to millimeter and sub-millimeter waves, to fulfill more demanding requirements on resolution, compactness and data rates. At these frequencies, the antennas have to be highly integrated with the electronic components, to facilitate the interconnection and avoid losses. Despite this need, integrated antennas have never showed good performance because of their intrinsic low efficiency. These antennas are limited by problems such as high surface-wave loss, narrow bandwidth and low front-to-back ratio [1].

Recently, an approach to greatly improve the efficiency of integrated antennas was proposed in [2], [3]. It consists of adding an artificial dielectric slab above the antenna in order to increase the front-to-back ratio. Because of the anisotropy of the artificial dielectric, surface waves are not excited, thus resulting in very high radiation efficiency.

A closed-form analysis of artificial dielectric layers (ADLs) was presented in [4], [5], valid for aligned layers (Fig. 1(a)), and subsequently generalized in [6] to include the shift between even and odd layers (Fig. 1(b)). The shift greatly increases the effective relative permittivity of the artificial dielectric with respect to the aligned case, thus it constitutes a key parameter for more flexible ADL designs.

All previous works considered lossless patches, made of perfect electric conductor. Losses in ADLs are typically very small because of the sub-wavelength dimensions of the patches, that yield very low current intensity on each patch. However, these losses can vary depending on how the ADL slab is illuminated, e.g. by a near source or under plane-wave incidence, and they also depend on the polarization and direction of the incident field [7]. For these reasons, it is useful to include the finite conductivity of the metal already in the analytical formulas, to accurately quantify the Ohmic dissipation in ADLs.

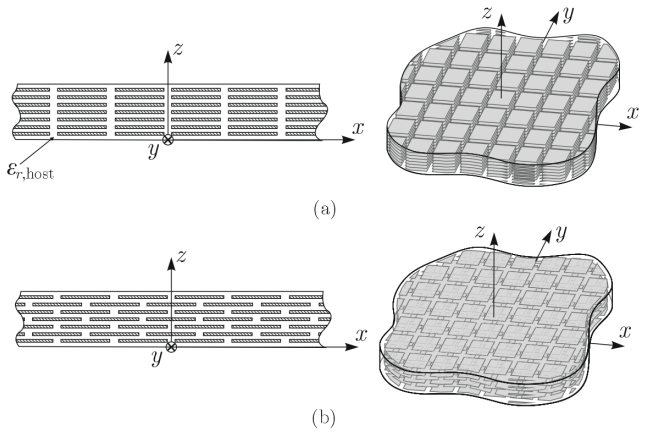

Fig. 1. Two-dimensional side view and three-dimensional prospective view for artificial dielectric slabs with (a) aligned and (b) shifted layers.

II. Multiple Layers with Finite Conductivity

We consider a plane wave incident on a finite cascade of layers with arbitrary shift between even and odd layers (indicated by s, equal along x and y), as shown in Fig. 2(a). Due to finite conductivity σ, the metal can be described by a surface impedance Z_s, which is given by

$$Z_s = (1+j)\sqrt{\frac{k_0\zeta_0}{2\sigma}} \tag{1}$$

where k_0 and ζ_0 are the free-space wavenumber and impedance, respectively.

By applying the equivalence theorem following a procedure similar to [8], an integral equation can be set up and solved with a procedure similar to [4]–[6]. The steps, omitted here for the sake of brevity, lead to the equivalent circuit representation in Fig. 2(b) can be used, where the admittances of the layers are separated into infinite-cascade and semi-infinite-cascade solutions, to describe the middle layers and the layers at the edges, respectively. The equivalent admittances terms, for transverse electric (TE) and transverse magnetic (TM) modes, are given by

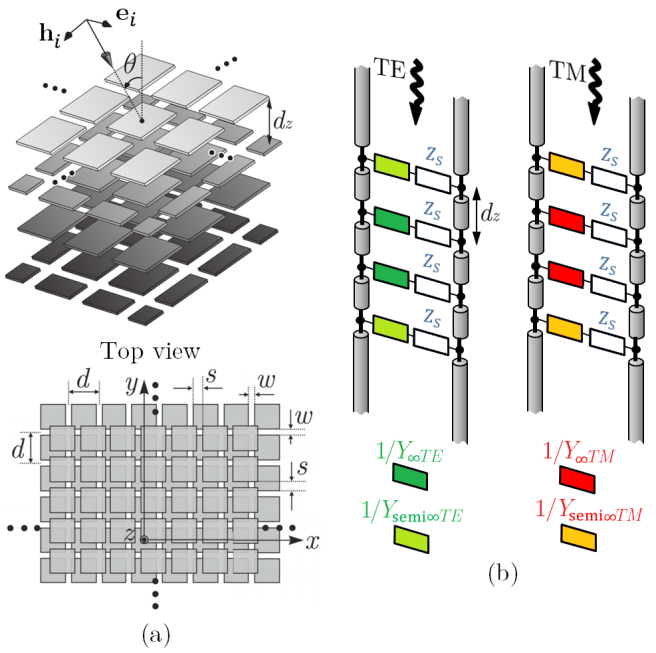

Fig. 2. Equivalent circuit representation of the ADL composed of 5 layers with finite conductivity for TE and TM component.

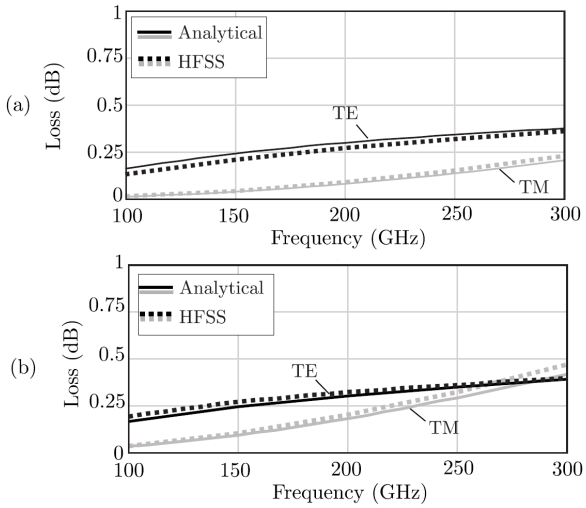

Fig. 3. Comparing losses calculated based on analytical solution and HFSS simulation. The plane wave is incident on a three-layer ADL with finite conductivity ($\sigma = 1000$ S/m) with angle of incidence $\theta = 60°$, $\phi = 0°$. The geometrical parameters are $d = 0.095\lambda_0$, $w = 0.01\lambda_0$, $d_z = 0.02\lambda_0$, with λ_0 being the wavelength at 300 GHz, and shift (a) $s = 0$ (aligned) and (b) $s = d/2$.

$$Y_{\infty TE} \approx 2 \sum_{m_y \neq 0} |\text{sinc}(k_{ym} w/2)|^2 S_\infty \left(\frac{k_{x0}^2}{2k_{ym}^2} \left(\frac{\zeta_0 k_0}{k_{zm}} + 2Z_s S_\infty \right)^{-1} + \left(\frac{\zeta_0 k_{zm}}{k_0} + 2Z_s S_\infty \right)^{-1} \right) \quad (2)$$

$$Y_{\infty TM} \approx 2 \sum_{m_x \neq 0} |\text{sinc}(k_{xm} w/2)|^2 S_\infty \left(\frac{k_{y0}^2}{k_{xm}^2} \left(\frac{\zeta_0 k_0}{k_{zm}} + 2Z_s S_\infty \right)^{-1} + \left(\frac{\zeta_0 k_{zm}}{k_0} + 2Z_s S_\infty \right)^{-1} \right) \quad (3)$$

where m_x and m_y are the indexes of the Floquet modes, $k_{xm} = k_{x0} - 2\pi m_x/d$ and $k_{ym} = k_{y0} - 2\pi m_y/d$ are the Floquet wavenumbers, which determine $k_{zm} = (k_0^2 - k_{xm}^2 - k_{ym}^2)^{1/2}$; $k_{x0} = k_0 \sin\theta\cos\phi$ and $k_{y0} = k_0 \sin\theta\sin\phi$ are the propagation constant of the incident plane wave along x and y, respectively.

The term S_∞ in (2) and (3) is given by

$$S_\infty = -j \cot\left(\frac{-j2\pi|m|d_z}{d}\right) + j e^{j2\pi m \frac{s}{d}} \csc\left(\frac{-j2\pi|m|d_z}{d}\right). \quad (4)$$

The admittances for the edge layers (first and last layer) have the same expressions, but replacing S_∞ with $S_{\text{semi}\infty}$:

$$S_{\text{semi}\infty} = \frac{1}{2} - \frac{j}{2} \cot\left(\frac{-j2\pi|m|d_z}{d}\right) + \frac{j}{2} e^{j2\pi m \frac{s}{d}} \csc\left(\frac{-j2\pi|m|d_z}{d}\right). \quad (5)$$

Full-wave HFSS simulations are made to validate the analytical solutions, and the comparison is shown in Fig. 3. A good agreement can be seen for the cases shown. Figures 3(a) and (b) refer to a cascade of three layers, aligned and shifted respectively. Since the losses of the structure with realistic conductivity values are negligible, an unrealistically low conductivity of $\sigma = 1000$ S/m is taken for the validation. The geometrical parameters are $d = 0.095\lambda_0$, $w = 0.01\lambda_0$ and $d_z = 0.02\lambda_0$, with λ_0 being the wavelength at 300 GHz. The incident plane wave is incoming at oblique angle ($\theta = 60°, \phi = 0°$).

REFERENCES

[1] D. Cavallo, W. H. Syed and A. Neto, "Artificial dielectric enabled antennas for high frequency radiation from integrated circuits," *11th Eur. Conf. Antennas Propagation*, Paris, 2017, pp. 1626-1628.

[2] W. H. Syed and A. Neto, "Front-to-back ratio enhancement of planar printed antennas by means of artificial dielectric layers," *IEEE Trans. Antennas Propag.*, vol. 61, no. 11, pp. 5408-5416, Nov. 2013.

[3] W. H. Syed, G. Fiorentino, D. Cavallo, M. Spirito, P. M. Sarro, and A. Neto, "Design, fabrication and measurement of 0.3 THz on-chip double-slot antenna enhanced by artificial dielectrics," *IEEE Trans. THz Sci. Tech.*, vol. 5, no. 2, pp. 288-298, Mar. 2015.

[4] D. Cavallo, W. H. Syed, and A. Neto, "Closed-form analysis of artificial dielectric layers—Part I: Properties of a single layer under plane-wave incidence," *IEEE Trans. Antennas Propag.*, vol. 62, no. 12, pp. 6256-6264, Dec. 2014.

[5] D. Cavallo, W. H. Syed, and A. Neto, "Closed-form analysis of artificial dielectric layers—Part II: Extension to multiple layers and arbitrary illumination," *IEEE Trans. Antennas Propag.*, vol. 62, no. 12, pp. 6265-6273, Dec. 2014.

[6] D. Cavallo and C. Felita, "Analytical formulas for artificial dielectrics with nonaligned layers," *IEEE Trans. Antennas Propag.*, vol. 65, no. 10, pp. 5303-5311, Oct. 2017.

[7] I. Awai, M. Furuta and T. Ishizaki, "Dissipation loss in artificial dielectrics," in *Proc. IEEE Antennas Propag. Soc. Int. Symp.*, Charleston, SC, 1-5 June 2009, pp. 1-4.

[8] M. Albani, A. Mazzinghi and A. Freni, "Rigorous MoM analysis of finite conductivity effects in RLSA antennas," *IEEE Transactions on Antennas and Propagation*, vol. 59, no. 11, pp. 4023-4032, Nov. 2011.